from the corresponding 1-D model (0.50%). However, both are small compared with calculations made over the past few years[1-4]. The currently calculated rate of change in global ozone is between −0.05 and −0.09% yr^{-1}, beginning in about 1970. This is, of course, for CFCs alone. Effects of opposite sign arising from the CO_2 increase and jet aircraft exhausts result in a combined effect on total ozone which is not significantly different from zero in recent 1-D model calculations[14].

The use of 2-D models to calculate potential ozone perturbations due to chemical releases of manmade origin provides a more detailed simulation of the real atmosphere than is possible with 1-D models. Various statistical techniques have been applied[15-18] to the analysis of ground-based ozone measurements made over the past 20 or more years in an attempt to detect trends suggested by 1-D models. Use of 2-D models allows the trend appropriate to a latitude region to be calculated, and information on changes in the seasonal variations as well as long-term trends can be used in the analysis. As noted above (Fig. 3*a*), the latitudinal variation in the present calculations of annual average ozone depletion is small, but the magnitude of the seasonal component increases towards the poles. Incorporating this additional information into analyses of ozone measurements may permit a better identification of any observed trend.

Accompanying a decrease in the amount of atmospheric ozone is an increase in the UV radiation reaching the Earth's surface. We have selected for a UV weighting function the action spectrum for DNA damage[19], which is one of the most sensitive to ozone changes. In general, changes in UV reaching the ground follow the total ozone column. In the steady state, for example, the yearly-averaged DNA-weighted UV dose is calculated to increase by 16%, essentially independent of latitude (Table 1). The largest percentage change occurs during the polar winter when the UV dose is smallest. The 2-D model gives an 'amplification factor', $\Delta UV/\Delta O_3 = 2.6$, while in the corresponding 1-D model this factor is 10% larger (2.8). Unlike calculations performed with previous chemical rate sets[4], we do not find a large variation of this amplification factor with latitude.

In the real atmosphere, more is changing than just the CFC concentrations. Prime examples are the CO_2 concentration, NO_x arising from conventional jet exhausts, and N_2O arising from the application of manmade fertilizers. While it is important to study the potential CFC effect in isolation as we have done here, 2-D models are approaching a degree of refinement where the estimation of multiple perturbations may become feasible. This type of investigation will be reported later.

Received 2 September; accepted 9 November 1981.

1. Hudson, R. D. & Reed, E. I. (eds) *The Stratosphere: Present and Future* (NASA RP-1049, 1979).
2. Panel on Stratospheric Chemistry and Transport *Stratospheric Ozone Depletion by Halocarbons: Chemistry and Transport* (National Academy of Sciences, Washington DC, 1979).
3. UK Department of the Environment *Chlorofluorocarbons and Their Effect on Stratospheric Ozone* (Pollution Paper No. 15, 1979).
4. Pyle, J. A. & Derwent, R. G. *Nature* **286,** 373–375 (1980).
5. Miller, C., Filkin, D. L., Owens, A. J., Steed, J. M. & Jesson, J. P. *J. geophys. Res.* **86** (in the press).
6. Miller, C., Steed, J. M., Filkin, D. L. & Jesson, J. P. *Nature* **288,** 461–464 (1980).
7. Ko, M. K. W., Livshits, M., Ryan, P. B. & Sze, N. D. *Status Report to Chemical Manufacturers Association for A.E.R. 2-D Model Project,* April (1981).
8. Pyle, J. A. & Rogers, C. F. *Nature* **287,** 711–714 (1980).
9. Andrews, D. G. & McIntyre, M. E. *J. Fluid Mech.* **89,** 609–646 (1978).
10. Dunkerton, T. *J. atmos. Sci.* **35,** 2325–2333 (1978).
11. Hudson, R. D., Reed, E. I. & Bojkov, R. D. (eds) *The Stratosphere 1981: Theory and Measurements* Appendix 1 (WMO/NASA, 1981).
12. Miller, C., Steed, J. M., Filkin, D. L. & Jesson, J. P. *Atmos. Envir.* **15,** 729–742 (1981).
13. Dutsch, H. *Adv. Geophys.* **15,** 219–322 (1971).
14. Penner, J. E. *Am. Geophys. Un. Fall Meet.,* San Francisco (1980); *IAMAP 3rd Scient. Assembly, Hamburg* (1981).
15. Hill, W. J., Sheldon, P. N. & Tiede, J. J. *Geophys. Res. Lett.* **4,** 21–24 (1977).
16. St John, D. S., Bailey, S. P., Fellner, W. H., Minor, J. M. & Snee, R. D. *J. geophys. Res.* **86,** 7299–7311 (1981).
17. Reinsel, G., Tiao, G. C., Wary, M. N., Lewis, R. & Nychka, D. *Atmos. Envir.* **15,** 1569–1577 (1981).
18. Bloomfield, P., Thompson, M. L., Watson, G. S. & Zeger, S. *Tech. Rep.* No. 182, Ser. 2 (Department of Statistics, Princeton University, 1981).
19. Setlow, R. B. *Proc. natn. Acad. Sci. USA* **71,** 3363–3366 (1974).

Electromagnetic jet-propulsion in the direction of current flow

Peter Graneau

MIT Francis Bitter National Magnet Laboratory, Cambridge, Massachusetts 02139, USA

Two simple experiments are reported here which demonstrate jet-propulsion in the direction of current flow between liquid and solid conductors. The observed effects seem to conform with Ampere's force-law, but no qualitative nor quantitative explanation has so far been found in terms of lorentzian forces and associated magnetohydrodynamics (MHD) phenomena. This research forms part of a wider investigation of the Ampere–Neumann electrodynamics and its relationship to modern science and technology.

In a classical experiment (Fig. 1) Ampere[1] claimed to have shown that, in addition to transverse forces on the conductor, the electric current creates repulsion between adjacent current-elements on the same straight line. He incorporated both transverse and longitudinal forces in his force-law (equation (1)). The longitudinal forces should place wires in tension and create relative motion between liquid and solid portions of a circuit. In Ampere's experiment the insulated or bare copper hairpin *cdefg* of Fig. 1, floating on two liquid mercury troughs *ab* and *a'b'*, will move towards *bb'* when sufficient current flows in and out of terminals *t* and *t'* connected with copper bars to the *a* and *a'* ends of the troughs. A transverse lorentzian force acts on the upturned hairpin bend *e*, but this should have its reaction force in the legs *cd* and *fg* of the hairpin, because the legs contain the source of the magnetic field at *e*. With action and reaction in the same rigid body, the Lorentz force at *e* should not be able to produce relative motion between hairpin and mercury. This point relating to Newton's third law has been argued strongly elsewhere[2-7].

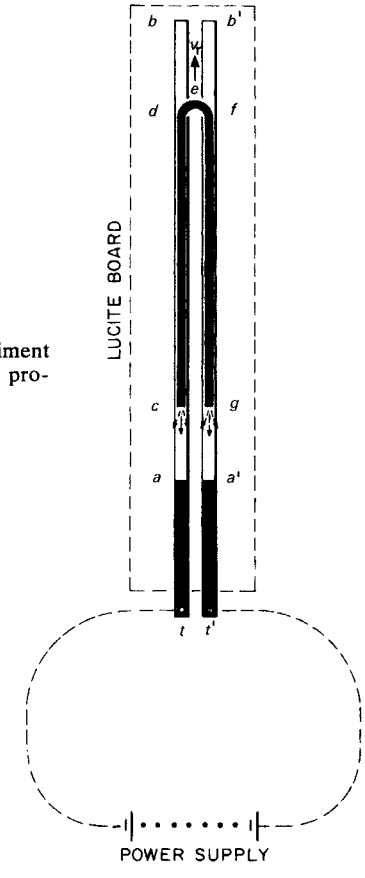

Fig. 1 Ampere's experiment demonstrating longitudinal propulsion.

0028–0836/82/040311—02$01.00

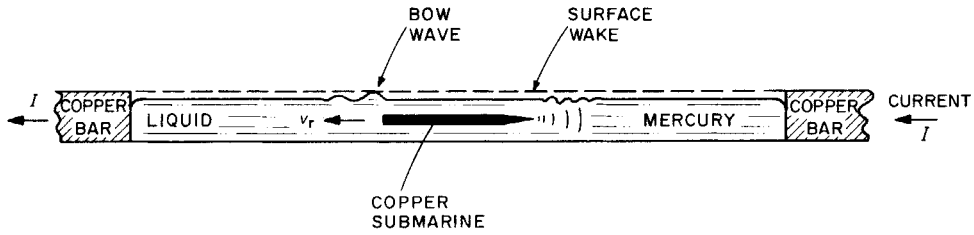

Fig. 2 Copper submarine experiment. Mercury trough length = 30 cm; cross-section 0.5 × 0.5 inch. Copper extension of troughs 30 cm long, 0.5 × 0.5 inch cross-section. Remote return circuit. $I = 400$ A. Copper submarine; 5 cm long, 3 mm diameter, 1 cm long taper. $v_r = 15$ cm s^{-1}.

Ampere did not mention that close to *c* and *g* liquid mercury moves relative to the trough walls and away from the ends of the hairpin. This motion confirms longitudinal propulsion, independent of any recourse to Newton's third law. The observation of this motion and the discovery of another longitudinal propulsion effect is now reported. While repeating Ampere's experiment, but mechanically blocking the forward motion of the hairpin, it was found that a wake formed in the liquid as though jets were mounted on the ends of the hairpin. A depression was detected in the liquid level close to *c* and *g*. When the hairpin ends were placed near to *a* and *a'*, liquid would well up on the copper walls and could be made to overflow. Short pieces of copper and stainless-steel wire laid on the mercury next to the hairpin ends were pushed away from *c* and *g*. Finally, a thin dielectric rod driven into the mercury near *c* or *g* and pivoted vertically above the point of immersion moved towards *a* or *a'*. These experimental facts leave little doubt that the longitudinal propulsion forces suggested by Ampere do exist. In showing that the net force of all amperian components on a rectangular circuit is zero, Cleveland[3] proved that longitudinal forces are of the same order of magnitude as transverse forces.

While trying to modify Neumann's[8] demonstration of longitudinal forces, I discovered another, even more remarkable propulsion arrangement. Figure 2 gives the details of this experiment. A copper 'submarine' consisting of a short piece of straight wire, squared off at one end and pointed at the other, has to be placed on the surface of a straight-through mercury trough conductor. When current is forced to flow along the trough, the transverse forces submerge the wire and longitudinal forces drive it along the centre of the trough until it strikes the solid copper bar. The wire travels with its blunt end forward. Its velocity is apparent from the bow wave on the liquid surface. The direction of travel does not depend on the direction of current flow and the experiment works equally well with 60-Hz alternating current.

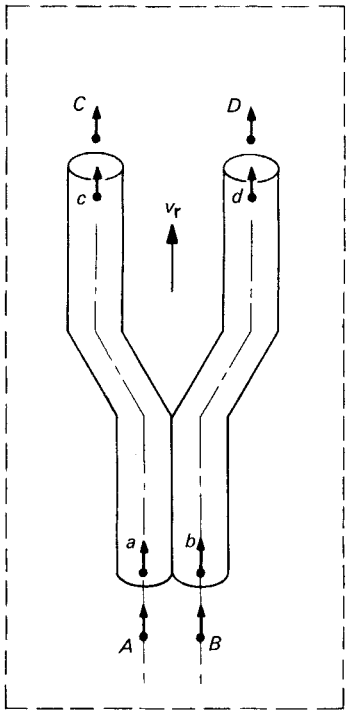

Fig. 3 Two-filament copper wishbone in liquid mercury bath.

Figure 3 explains the amperian submarine propulsion mechanism. This simplified representation shows a wishbone made of two solid current filaments immersed in liquid metal. Only two sets of four current-elements are considered. One set is *a*, *b*, *c* and *d* located in the ends of the wishbone filaments. The other four, *A*, *B*, *C* and *D* are adjacent in-line elements in the liquid. The Ampere force $\Delta F_{m,n}$ in dyn between two current-elements at points *m* and *n* of lengths d*m* and d*n* and separated by the distance $r_{m,n}$ is given by

$$\Delta F_{m,n} = -i_m i_n (\mathrm{d}m \cdot \mathrm{d}n / r^2_{m,n})(2\cos\varepsilon - 3\cos\alpha\cos\beta) \quad (1)$$

where i_m and i_n are the element currents in absolute ampere, ε is the angle of inclination between the elements, and α and β are the angles which the elements make with the distance vector $\mathbf{r}_{m,n}$. When the force is positive it represents repulsion and when negative it represents attraction. Using this law to compute the repulsion between solid and liquid elements at one end of the wishbone and then at the other, it can easily be shown that the solid object is being pushed relative to the liquid in the direction of the velocity v_r indicated on Fig. 3. According to Ampere's law, therefore, it is the current concentration in the pointed end of the wire which is responsible for the propulsion of the copper submarine of Fig. 2.

So far the longitudinal propulsion mechanism has not been explained in terms of relativistic field theory and associated MHD effects. In view of the widespread acceptance of Ampere's force law during the nineteenth century and its implications with regard to solid-state physics and MHD technology, I urge others to repeat these simple experiments and comment on their observations.

This research was sponsored by NSF.

Received 27 October; accepted 26 November 1981.

1. Ampere, A. M. *Memoires sur l'Electrodynamic* Vol. 1, 25 (Gauthier-Villars, Paris, 1885).
2. Bush, V. *J. Math. Phys.* **5**, 129 (1926).
3. Cleveland, F. F. *Phil. Mag.* **25**, 416 (1936).
4. O'Rahilly, A. *Electromagnetic Theory* Vol. 1, 102 (Dover, New York, 1965).
5. Whittaker, E. *History of the Theories of Aether and Electricity* Vol. 1, 84 (Thomas Nelson, London, 1951).
6. Robertson, I. A. *Phil. Mag.* **36**, 32 (1945).
7. Rosser, W. G. V. *Contemp. Phys.* **3**, 28 (1961).
8. Neumann, F. E. *Vorlesungen ueber Elektrische Stroeme*, 102 (Teubner, Leipzig, 1884).

A composite semiconductor photoanode for water electrolysis

Yoshihiro Nakato, Nobuyuki Takamori & Hiroshi Tsubomura

Department of Chemistry, Faculty of Engineering Science, Osaka University, Toyonaka, Osaka 560, Japan

Photoelectrolysis of water by means of semiconductor photoelectrochemical cells has attracted much attention from the point of view of solar energy conversion[1–5]. Metal oxides such as TiO_2, WO_3, or Fe_2O_3 act as stable photoanodes, but they need an external bias for the photodecomposition of water to compensate for their too low surface band energies. We report here that water can be photodecomposed effectively without external bias by using a semiconductor/redox electrolyte/semiconductor junction (SES) as the photoanode.

The structure of the SES is indicated in Fig. 1. It consists of single crystal wafers of n-CdS and n-TiO_2 (0.3–0.7 mm thick)

0028–0836/82/040312—02$01.00